α-element enhanced opacity tables and low-mass metal-rich stellar models*

A. Weiss[1], M. Salaris[2,1], J.W. Ferguson[3], and D.R. Alexander[3]

[1] Max-Planck-Institut für Astrophysik, Karl-Schwarzschild-Str. 1, 85748 Garching, Federal Republic of Germany
[2] Astrophysics Research Institute, Liverpool John Moores University, Twelve Quays House, Egerton Wharf, Birkenhead, CH41 1LD, UK
[3] Physics Department, Wichita State University, Wichita, KS 67260-0032, USA

ABSTRACT

Context. Calculation of stellar models with varying degrees of α-element enhancement.
Aims. We investigate the influence of both a new generation of low-temperature opacities and of various amounts of α-element enhancements on stellar evolution models.
Methods. New stellar models with two different α-element mixtures and two sets of appropriate opacity tables are computed and compared. The influence of the different mixtures as well as that of the improved generation of opacity tables is investigated.
Results. It is found that around solar metallicity the new opacity tables have a drastic influence on stellar temperatures, which is mainly an effect of the new low-temperature tables, and not of variations in α-element enhancement factors. The latter, however, influence stellar lifetimes via systematic opacity effects at core temperatures. We trace the reason for the low-temperature table changes to errors in the old tables.
Conclusions. Variations in α-element abundance ratios affect the main-sequence properties of super-solar metallicity stars significantly. Red giant branch effective temperatures depend only slightly on the specific mixture. Our older low-temperature opacity tables were shown to be erroneous and should no longer be used for stellar models with near- or super-solar metallicity. Corrected tables have already been produced.

Key words. Stars: interiors – evolution – abundances – low-mass

---

* submtitted for publication to Astronomy & Astrophysics

1. Introduction

It is now widely accepted that the chemical composition of stars can be classified by two main classes of metal mixtures: one with nearly solar metal ratios and another one, in which the so-called α-elements are enriched, while most other elements, in particular C, N, and those of the iron-group, are present in near-solar element ratios. The α-elements are those produced by α-captures on oxygen in Supernova II explosions; they are O, Ne, Mg, Ca, Si, Ti. These elements are enhanced over their solar relative number fractions by factors of 1.5-3 (or 0.2-0.5 dex on a logarithmic scale). Since oxygen is contributing around 50% of the metals, its α-enhancement can significantly increase the total metallicity. Using one element, in particular iron, as the metal indicator, can therefore be misleading in evaluating the total metallicity of stars. In the traditional picture of galactic populations, Pop I is characterized by a solar metal mixture, while Pop II shows significant α-enhancement. However, the correlation with total metallicity or [Fe/H] is not at all a strict one, since the relative α-element abundances depend on the star formation history and rate. It is known that in elliptical galaxies and possibly the galactic bulge stellar compositions with solar or super-solar iron abundances and strong α-enhancement exist, indicating intensive and short-lived star formation histories. For a discussion of α-element evolution and its connection with galacto-chemical evolution, see the review by Wheeler et al. (1989).

Calculation of stellar models therefore requires for each value of total metallicity (Z) at least these two basic internal metallicity mixtures: a solar-scaled and an α-enhanced one. This requirement has been realized in the early nineties and since then the number of stellar libraries which also take into account α-enhancement has steadily increased. While the inclusion of individual element abundances is trivial for the nuclear energy generation, it is non-trivial for an elaborate equation of state and for opacities. In the former case, one trusts that as long as hydrogen and helium are dominating the gas, the individual element abundances within the metals is of negligible influence. However, for the opacities this no longer holds true since the various elements contribute very differently to the total absorption. As the calculation of opacities has developed into a specialised branch, this requires separate calculations by groups active in this field or flexible programs for end-users.

In the past we have tried to include α-enhancement in the opacity tables we used as best as possible. In Bencivenni et al. (1989) an α-enriched mixture was first taken into account using the Los Alamos Astrophysical opacity library (Huebner et al. 1977) for temperatures above 1 eV. Similar tables were used in Weiss et al. (1995), where for the first time α-enhanced stellar models for elliptical galaxies were calculated with almost consistent input physics. However, at low temperature the opacities were still solar-scaled. While it was shown by Salaris et al. (1993) that at low metallicities opacities with solar-scaled abundances and essentially the same total metallicity are presumably a good replacement for α-enhanced tables, this could not be assumed for near-solar or even super-solar metallicities. The final step became possible when low-temperature opacity tables, which include molecular absorption processe,s were made available by Alexander & Ferguson (1994, AF94), both for solar and α-enhanced metal mixtures. These could then be combined with high-temperature tables for *completely identical* mixtures from (Iglesias & Rogers 1996, OPAL; IR96). The enhancement for the various α-elements are variable in this metal mixture (Salaris & Weiss 1998). These tables were used by the authors for globular cluster calculations (Salaris & Weiss 1998) demonstrating also that the approximation by Salaris et al. (1993) begins to fail around [Fe/H] = -0.7, the iron content of 47 Tuc. A complete set of models with metallicities ranging from $Z = 0.008$ to 0.070 using the same opacity tables was added to the Padova stellar library by Salasnich et al. (2000). Similar, but independent opacity tables from the same sources were used, e.g., in the models by the Victoria and Yale-Yongsei groups (VandenBerg et al. 2000; Yi et al. 2003). Here, all α-elements have been enhanced by the same factor, ranging in the different sets from 0.3 to 0.6 dex.

As demonstrated first by Salaris et al. (1993), and verified by, e.g., Salaris & Weiss (1998) and VandenBerg et al. (2000), to first order α-enhanced opacities at low metallicity and for low mass stellar models can be replaced by scaled-solar ones for the same metal fraction Z, provided that the ratio $(X_\mathrm{C}+X_\mathrm{N}+X_\mathrm{O}+X_\mathrm{Ne})/(X_\mathrm{Mg}+X_\mathrm{Si}+X_\mathrm{S}+X_\mathrm{Ca}+X_\mathrm{Fe})$ – where X_i denotes the mass fraction of element i – is approximately the same in both mixtures (in spectroscopic notation this corresponds to $[(X_\mathrm{C}+X_\mathrm{N}+X_\mathrm{O}+X_\mathrm{Ne})/(X_\mathrm{Mg}+X_\mathrm{Si}+X_\mathrm{S}+X_\mathrm{Ca}+X_\mathrm{Fe})] \sim 0$). As a consequence, differences in the internal distribution of α-elements are of minor significance, as long as this condition is satisfied. The extension of this result to solar or super-solar metallicities has however never been investigated.

For a population synthesis project (Coelho et al. 2006, in preparation), we decided to compare stellar models of low-mass stars using the previously introduced α-enhanced tables with varying enhancement factors to other models with new opacity tables, in which all α-elements are enhanced by a constant factor of 0.4 dex. The individual metal abundances are listed in Table 1 and provide $[(X_\mathrm{C}+X_\mathrm{N}+X_\mathrm{O}+X_\mathrm{Ne})/(X_\mathrm{Mg}+X_\mathrm{Si}+X_\mathrm{S}+$

$X_{Ca} + X_{Fe})] = 0.14$ in case of the variable enhancement mixture, and 0.007 for the constant enhancement one. The total metallicity ranges from $Z = 0.011$ to 0.048. For the calculation of the latter tables the new low-temperature molecular opacity code by Ferguson et al. (2005, FA05) and for the high-temperature regime the OPAL online calculation of opacity tables[1] were used. We therefore are faced with the fact that the new tables (for $\log T \leq 4.5$; but used only for $\log T \leq 4.1$) differ from the old ones both in the internal metal distribution ("mixture effect") and in the method of calculation ("generation effect"). For the higher temperatures only the mixture effect is present.

The purpose of the present paper is to present new low-mass stellar models up to the red giant tip and the influence of variations in α-enhancement on the evolution at given total super-solar metallicity. Second, we investigate the influence of the new low-temperature opacities and that of a variation of internal element distributions in these tables. This is an important issue because of the fact that one cannot expect to have always opacities at hand which are fully consistent with the mixture chosen for the stellar models. For completeness, we also discuss metal-poor cases.

The stellar models and the sets of opacity tables are introduced in Sect. 2. The basic results of the calculations and various tests are the subject of Sect. 3. The low-metallicity case follows in Sect. 5, before the discussion and conclusions close the paper in the final section.

2. Model details

2.1. Stellar evolution program

The stellar models were calculated with the Garching stellar evolution code, which was described in Weiss & Schlattl (2000) and lately in Weiss et al. (2005). We will concentrate here on the description of the opacity tables. Our code uses tables of Rosseland mean opacities κ for mixtures quantified by the mass fractions of hydrogen and metals (both ranging from 0 to 1; in total of order 80), and with a temperature and density grid of about 85 and 25 grid points[2]. The interpolation in this grid is done by a two-dimensional, bi-rational spline algorithm (Spaeth 1973). In mixture we use parabolic polynomials first in X (hydrogen) between the three tables closest to the actual value, and then in $\log Z$ (metallicity). In practice, and as long as the total metallicity is not changing, e.g. either by advanced nuclear burning phases or metal diffusion, tables for only three metallicity values are sufficient for the whole calculation. For evolutionary stages from core helium burning on, we have special core tables, but these are not of interest for the present work.

The tables themselves are the end product of the merging of source data. We have four main regions in the $T - R$ domain:

- $\log T < 3.8$, for which we use the Wichita State Alexander & Ferguson molecular opacity tables mentioned in the introduction
- $8.7 > \log T > 4.1$, for which OPAL tables are used
- high density: here we employ the results by Itoh et al. (1983) for electron conduction opacities
- $\log T > 8.7$, for which no OPAL data are available; here we use the old Los Alamos Opacity Library (see Sect. 1; in the present case this is irrelevant).

In between these regions are transitions. Between $3.8 < \log T < 4.1$, where both Wichita State and OPAL data are available, we have a linear transition in $\log \kappa$ along with $\log T$ from one source to the other. The agreement between both tables is excellent and the transition is very smooth. At the high-density edge we add radiative (κ_r) and conductive (κ_c) opacities according to

$$1/\kappa = 1/\kappa_r + 1/\kappa_c.$$

Since with increasing density κ_c is dominating, the radiative contribution can be omitted once $\kappa_r > \kappa_c$. However, in particular at $\log T < 5$ the radiative tables end before this situation is reached. In case the gap between the end of the radiative opacity table and the density from which on κ_c is already lower than the last radiative value available is only 1-2 dex, we boldly interpolate over this gap (cubic spline). If the gap is too large, the final κ-table has to end here. Should we run out of the table definition range during the stellar model calculations, we use the last table value. This happens at isolated points in some low-mass main-sequence envelopes and cannot be avoided as long as the input tables do not cover the full $\rho - T$-plane.

All our tables are constructed in this same way in a separate step before they are used by the stellar evolution code.

[1] `http://www-phys.llnl.gov/Research/OPAL`

[2] As the density coordinate we actually use the usual $\log R = \log \rho - 3 \log T + 18$

Table 1. Chemical abundances of the metals. Columns 2 and 3 contain the standard Grevesse & Sauval (1998) solar abundances on a logarithmic scale where the hydrogen abundance is 12.00 and as relative mass fractions. Columns 3 and 4 show the abundances of the α-enhanced mixture by Salaris & Weiss (1998, "α-v") and columns 5 and 6 for a constant α-enhancement of 0.4 dex ("α-c"). α-elements are printed in italics.

el.	solar		α-v		α-c	
C	8.52	0.173344	8.52	0.076535	8.52	0.083953
N	7.92	0.053187	7.92	0.023483	7.92	0.024600
O	8.83	0.482487	9.33	0.673656	9.23	0.573606
Ne	8.08	0.096446	8.37	0.083031	8.48	0.128651
Na	6.33	0.001999	6.33	0.000883	6.33	0.001038
Mg	7.58	0.037597	7.98	0.041697	7.98	0.049009
Al	6.47	0.003599	6.47	0.001589	6.47	0.001868
Si	7.55	0.040543	7.85	0.035717	7.95	0.052850
P	5.45	0.000355	5.45	0.000157	5.45	0.000184
S	7.33	0.021158	7.66	0.019972	7.73	0.036357
Cl	5.50	0.000456	5.50	0.000201	5.50	0.000237
Ar	6.40	0.005380	6.40	0.002375	6.40	0.002118
K	5.12	0.000210	5.12	0.000093	5.12	0.000109
Ca	6.36	0.003735	6.86	0.005215	6.76	0.004869
Ti	5.02	0.000204	5.65	0.000384	5.42	0.000266
Cr	5.67	0.000989	5.67	0.000437	5.67	0.000513
Mn	5.39	0.000549	5.39	0.000242	5.39	0.000285
Fe	7.50	0.073517	7.50	0.032459	7.50	0.037284
Ni	6.25	0.004246	6.25	0.001874	6.25	0.002203

2.2. Stellar models

For the larger project about stellar population synthesis (Coelho et al. 2006, in preparation) we calculated mixtures of varying metallicity from $Z = 0.005$ to 0.048, but in the present paper we will be concentrating on one mixture, which is $X = 0.679, Z = 0.032$. All α-elements are enhanced over the solar-scaled abundances by 0.4 dex, for which we used the solar mixture by Grevesse & Sauval (1998). For comparison with a solar-scaled mixture with identical [Fe/H] models with the mixture $X = 0.735$, $Z = 0.017$ was chosen; the higher total metallicity is thus assumed to be connected with an increase in helium abundance. In mass our models cover the range from 0.6 to 1.2 $M_\odot$ in steps of 0.05 $M_\odot$. Our calculations start with the zero-age main-sequence (ZAMS) defined by homogeneous stellar composition and vanishing gravo-thermal energies in the initial model. Since this composition is not identical to nuclear equilibrium in the core (^{3}He, CNO-isotopes) the initial few million years are spent to adjust the composition accordingly. This leads to a well-known short loop around the ZAMS position, which will be visible in some of the diagrams. We follow the evolution into the core helium flash at the tip of the RGB, until the helium luminosity is of order 1000 $L_\odot$.

We emphasize that the chemical composition in the models is always the same (α-c), as given in Table 1. What is varied in the calculations presented below, is just the internal composition of the opacity tables.

2.3. Opacity tables

The first set of models (A) was calculated with the same opacity tables as those used by Salaris & Weiss (1998) and Salasnich et al. (2000), which are a combination of OPAL and Wichita State opacities for the α-v mixture[3] They were calculated at the time when the new Wichita State low-temperature molecular opacities (Ferguson et al. 2005) were not yet available, in particular not for non-solar metal compositions, and under the assumption that the slightly different table composition would not influence the model properties significantly, such that this internal inconsistency could be tolerated.

Set B followed after low-T tables for mixture α-c had been calculated. High-T OPAL tables were obtained from the OPAL-website for the identical mixture. This is the most recent set of opacity tables and fully consistent with the model compositions. The models for the population synthesis project (Coelho et al. 2006, in preparation) have been computed with it.

[3] These tables were originally provided by F. Rogers and D. Alexander by private communication (1994/1995), but later made public on the respective websites, `http://www-phys.llnl.gov/Research/OPAL` and `http://webs.wichita.edu/physics/opacity/`.

Table 2. Details about the tables of Rosseland mean opacities for the various sets of stellar models. Low- and high-temperature ranges are as described in Sect. 2.1. Mixture labels are as in Table 1 and "code" entries refer to the relevant publication, where the calculation method and details are described. "AF05" refers to a re-computation in 2005 using the original AF94 program.

	low-T		high-T	
Set	mix	code	mix	code
A	α-v	AF94	α-v	IR96
B	α-c	FA05	α-c	IR96
T1	α-c	FA05	α-v	IR96
T2	α-v	AF94	α-c	IR96
T3	α-v	FA05	α-c	IR96
R	α-v	AF05	α-v	IR96

To analyse the results of the following section, additional sets of tables were produced for various test cases. They consist of *inconsistent* combinations of low- and high-T tables and are listed in Table 2 as well. The final case R is a repetition of case A, but the tables were recomputed with the same code by Ferguson et al. (2005).

3. Results

3.1. From old to new (Case A to B)

The scientifically interesting question is how much the use of opacity tables with an internal α-element distribution (α-v) differing from that of the models themselves (α-c) influences the evolution. This is an interesting aspect of stellar modelling as long as hghly accurate opacities cannot be calculated on-line with the models. To evaluate this, we computed cases A and B, the latter being the fully consistent one. We emphasize again that the model composition in case A is the same as in B, but that the internal metal distribution of the opacity tables is slightly different. The resulting tracks are shown in Fig. 1. The effect is drastic: for the 0.9 $M_\odot$ model, ZAMS and TO-positions are 0.08 resp. 0.06 dex brighter, the turn-off (TO) also being 0.02 dex cooler and the main-sequence lifetime is 3.3 Gyr shorter than that for case B (17.8 Gyr). RGB temperatures are higher by $\approx$ 250 K, too. Theses changes are also typical for all other masses.

In the tracks, small kinks are visible both on the main sequence and on the subgiant branch. The reason is that in the phase lying between these points the OPAL equation of state (Rogers et al. 1996) does not cover the conditions in the outer stellar envelope and we switch back to a simple Saha-type equation of state. This effect is less pronounced for lower stellar masses. We have repeated a few cases using the new OPAL-based equation of state by Irwin (described in Cassisi et al. 2003), which is more extended. The tracks from this repeated calculation agree extremely well with those shown, but in addition are smooth without any kinks.

Since the strong influence of the different α-enriched opacity tables could be due to either the generation or the composition effect, or both, we set out to isolate this by additional tests in which we used specific opacity tables with only one effect being present.

3.2. T1: new low-T opacities

For this test case we used only the low-T opacity tables for the α-c mixture. The high-T tables are still those for mixture α-v as in case A. Figure 2 shows the resulting tracks for three different masses. Temperatures along the RGB (for $M = 0.8$ and $1.0\,M_\odot$) are again lower by more than 200 K for the new low-T tables, while the ZAMS and TO luminosities differ only by a few hundreths of a magnitude. Correspondingly, main-sequence lifetimes agree within 0.4 Gyr (0.8 $M_\odot$ and 1.0 $M_\odot$). The new low-T opacities apparently affect the envelope structure significantly, while the high-T tables with the new mixture do influence the core properties.

3.3. T2: new high-T mixture

Since the method for calculating the OPAL opacities has not changed, replacing the high-T tables with those for the new mixture does not imply a generation effect. Again, we show the comparison between case A and this test case (T2) in Fig. 3. Since the low-T opacities are now identical, the RGB temperatures completely agree. However, changes on the main-sequence remain. The ZAMS luminosity is lower by 0.07 dex in case

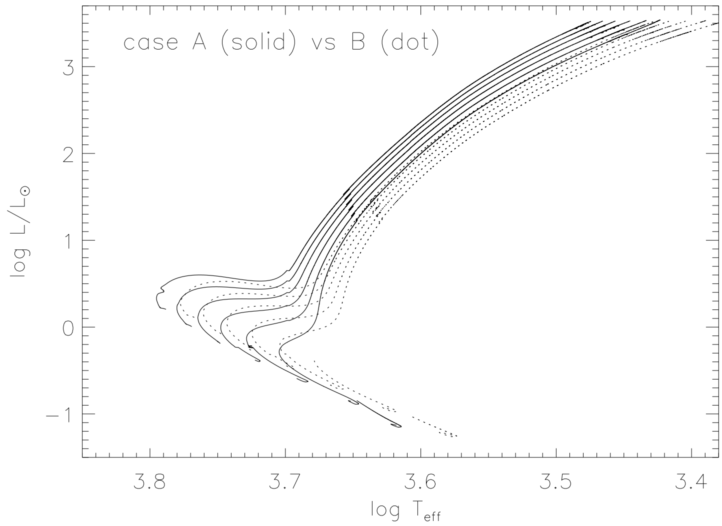

Fig. 1. Comparison of evolutionary tracks for cases A and B. Masses range from 0.6 $M_{\odot}$ to 1.2 $M_{\odot}$ in steps of 0.1 $M_{\odot}$ (we omitted the intermediate mass values). The calculations were stopped either at the RGB tip or if the age exceeded 50 Gyr. For this reason the tracks do not extend to the RGB for $M = 0.60\,M_{\odot}$ for case A, and $M = 0.60\,M_{\odot}$ and $0.70\,M_{\odot}$ for case B. The composition of both model sets is identical (α-c), but that of the opacity tables is not.

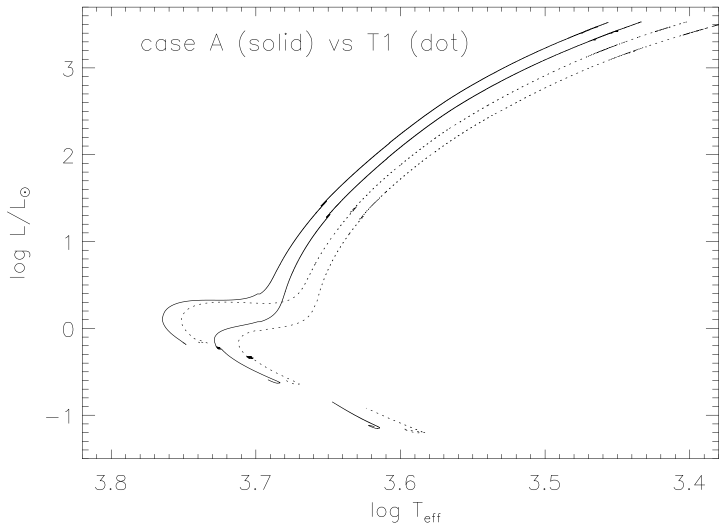

Fig. 2. Comparison of evolutionary tracks for cases A and T1. Masses are 0.6, 0.8 and 1.0 $M_{\odot}$.

T2 ($M = 0.80\,M_{\odot}$), and the MS lifetime longer by 4.3 Gyr. The reason for this effect is evident from Fig. 4, where we show a contour plot of the ratio of Rosseland opacities between the old and new composition. Over a wide temperature and density range, typical for core temperatures of main sequence stars the α-c opacities are higher by 5-20%. The differences are very similar also for lower helium content. An increase in opacity, as is well known, leads to a lower luminosity and thus a longer burning time.

3.4. T3: new generation of low-T tables

After we identified the main influence of low- and high-T tables, when going from case A to B, we are separating generation- from mixture effect for the low-temperature opacities. To this end, tables for mixture α-v were calculated using the method of Ferguson et al. (2005) and combined with the α-c OPAL tables. We thus

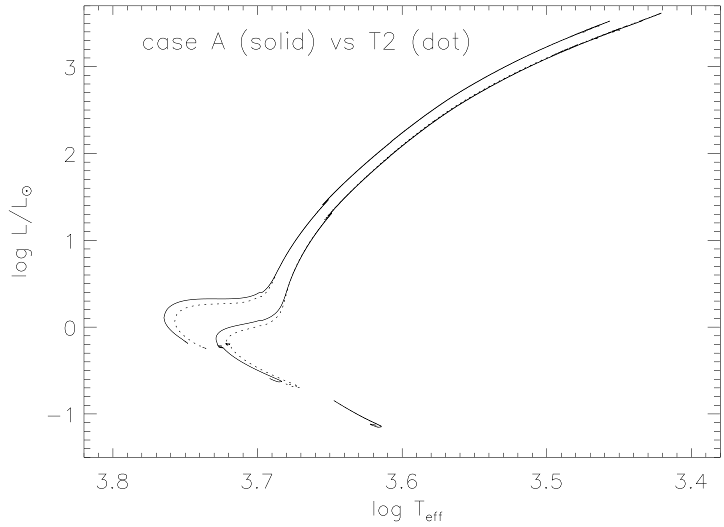

Fig. 3. Comparison of evolutionary tracks for cases A and T2. Masses are 0.6, 0.8 and 1.0 $M_{\odot}$.

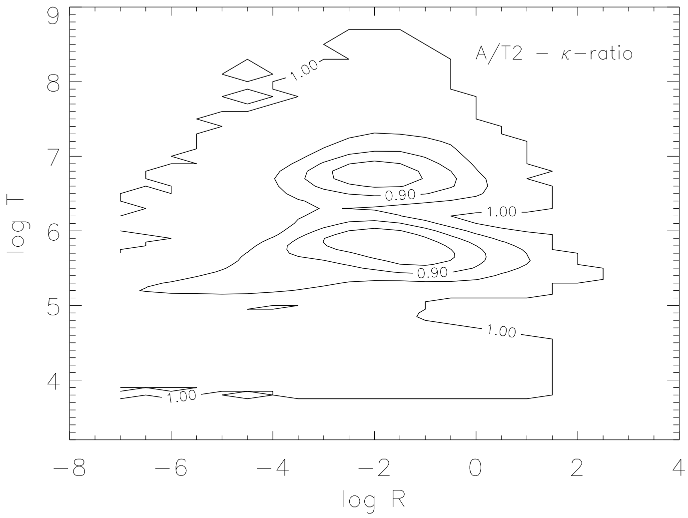

Fig. 4. Ratio of Rosseland opacities κ between a typical table used in cases A and T2. The composition is $X = 0.700$, $Z = 0.03$. Shown are isocontours of the ratio.

compare to case B, with only the mixture-effect at low temperatures present, shown in Fig. 5. Obviously, in spite of employing mixture α-v for the molecular opacities, the track resembles that of case B, the completely consistent α-c calculation, very much. In fact, for $M = 0.80$ and $1.0\,M_{\odot}$ ZAMS luminosities agree within 0.003 dex, TO luminosities and effective temperatures better than 0.004 resp. 0.003 dex, and RGB tip temperatures better than 0.09 dex. The TO and RGB tip ages are within 100 Myr. The conclusion from this experiment and the one of Sect. 3.2 is therefore that for the low-temperature opacities the generation effect is the dominating one and that within the same generation of tables the mixture effect is almost negligible. This is different from the effect on the atomic opacities of the interior (Sect. 3.3).

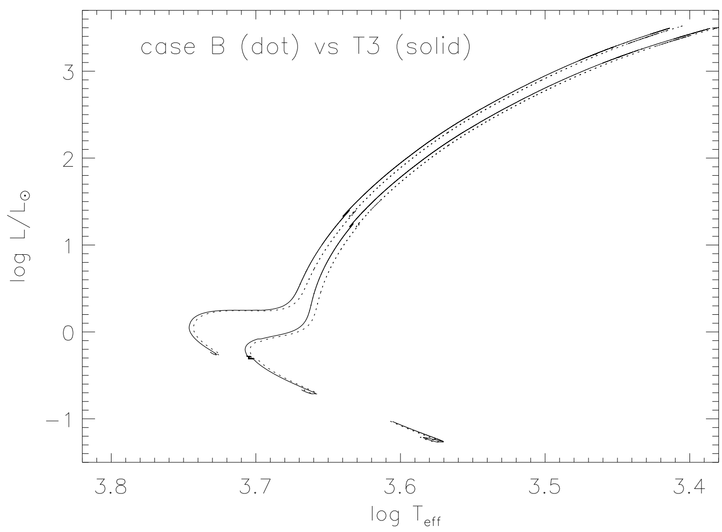

Fig. 5. Comparison of evolutionary tracks for cases B (dotted lines) and T3 (solid) for masses of 0.6, 0.8, and 1.0 $M_\odot$.

3.5. R: low-T tables recalculated

The result of Sect. 3.4 is quite surprising given the fact that Ferguson et al. (2005) reported rather small changes in the new molecular opacities for solar-type mixtures. To verify this conclusion further, we investigated the low-temperature tables for α-v mixtures in more detail. A comparison displayed quite large differences of ±10% around $\log T \approx 3.6$, increasing further to lower temperatures. Fig. 6 shows a sample comparison at $\log R = -3$ for the mixture $X = 0.7$, $Z = 0.02$ between the old AF94 and the new FA05 table. For $\log T \lesssim 3.4$ the difference in fact increases up to a factor of 3. This finding emphasizes that the new calculation programs alone are responsible for the change in opacities. Using these recalculated FA05 tables for mixture α-v, combined with the corresponding high-T OPAL tables, we show the comparison of this case R, which is the “2005 update” of A, with case B in Fig. 7. We thus see here the effect of changing the α-element enhancement factors within the opacity tables, which, however, were calculated with the same program in both cases. Obviously, along the RGB the two cases agree very closely, while the differences in the earlier evolutionary phases is that of Sect. 3.3 and Fig. 3.

3.6. α-enhanced low-T tables of 1994

In contrast to the solar metallicity case investigated in Ferguson et al. (2005), the re-calculation of the α-v low-temperature tables with the new molecular opacity code revealed the large changes of Fig. 6, in particular at $T \lesssim 2500$ K. The original calculations by D. Alexander (1994, private communication to A. Weiss) were therefore repeated with the original code of Alexander & Ferguson (1994). The result is also displayed in Fig. 6 as the dashed line, and differs strongly from the original 1994 result, shown as the dotted line, in the temperature region between $3.25 \lesssim \log T \lesssim 3.35$, while it agrees very well with the result from the new code, at least down to $\log T \approx 3.15$, below which the differences can be explained by by updated grain physics, e.g. more grain species in the equation of state and updated grain opacities, in FA05.

The conclusion is that an error was made in the original calculations provided to A. Weiss in 1994. This error was essentially a series of typos in the input abundances to the opacity tables run at that time. *The α-enhanced tables used in several publications (Salaris & Weiss 1998; Weiss & Schlattl 2000; Salasnich et al. 2000, and others) are therefore erroneous and should not be used any longer.* At least at solar and super-solar metallicities they influence the effective temperatures of the models strongly by the underestimation of the opacity at low temperatures: Red Giant models are rendered too blue. Similar opacity tables for different α-enhancement factors calculated with the same code and used, e.g. in VandenBerg et al. (2000) and Yi et al. (2003), do not suffer from this error. We also emphasize that most of the papers using the erroneous tables dealt with significantly lower total metallicity at which the models are much less sensitive (see below).

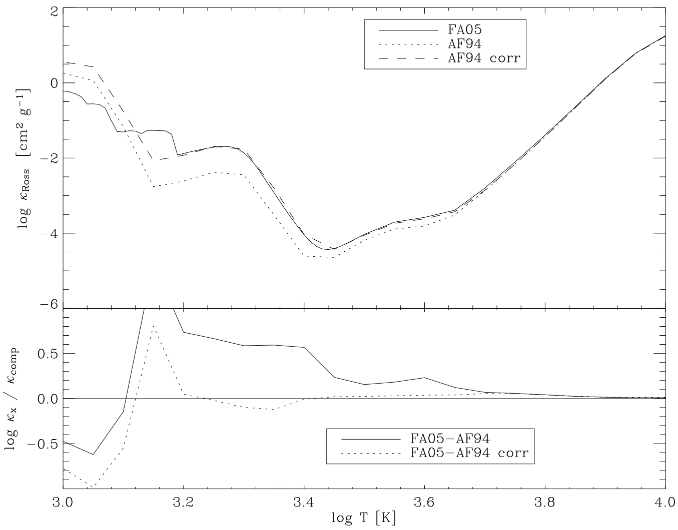

Fig. 6. Comparison of Rosseland mean opacities in a table with mixture $X = 0.7$, $Z = 0.02$, taken at $\log R = -3$ as function of temperature (upper panel). Lower panel: differences in $\log \kappa$. F05 denotes the new calculation of tables for the same $\alpha - \nu$ element ratios as in the original AF94 table.

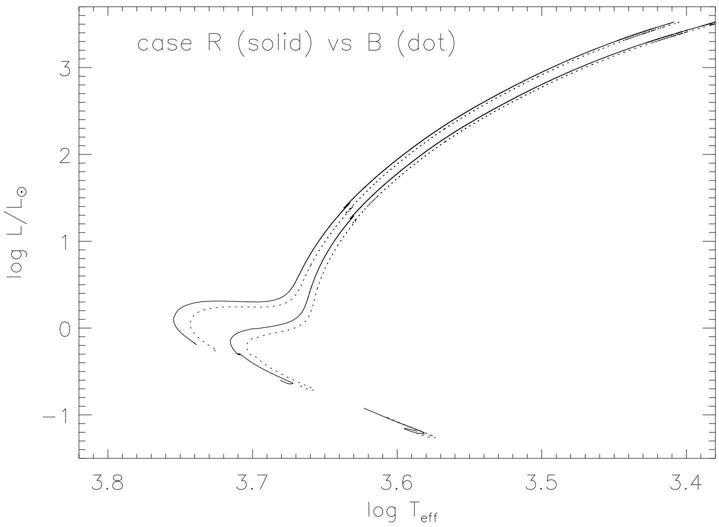

Fig. 7. Comparison of evolutionary tracks for cases B and R. Masses are 0.6, 0.8 and 1.0 $M_\odot$.

4. Low-metallicity models

Figure 8 shows the same opacity comparison between α-c ("f05") and α-v tables, the latter for the new ("af94 corr") and original ("af94 old") calculation, for $Z = 0.0001$. The situation resembles that of Fig. 6, but the opacity itself is lower by an order of magnitude. All changes should therefore result in milder effects on the stellar models.

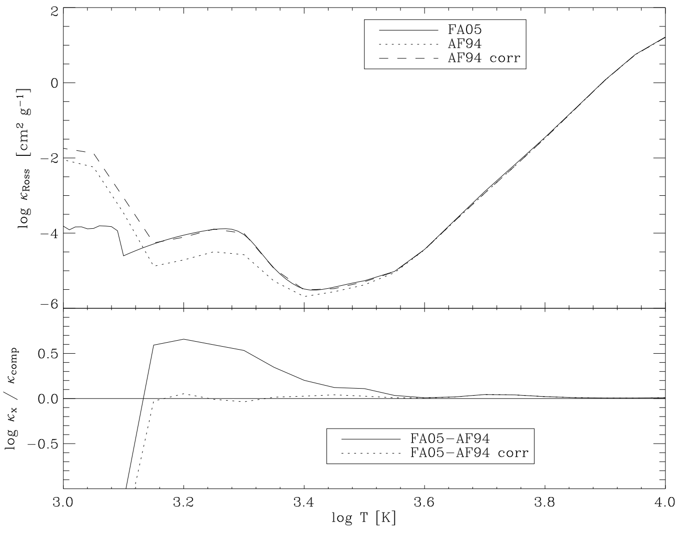

Fig. 8. As Fig. 6, but for $Z = 0.0001$.

Indeed, Fig. 9 (lower panel) demonstrates this for the case of $M = 0.8\,M_\odot$, and $Z = 0.001$: The track labelled "AF94" was calculated with the original α-enhanced table and corresponds to the tracks used in, e.g. Salaris & Weiss (1998). The same code as in this paper was used, too. Employing the newly calculated opacities (F05) again results in a cooler RGB; all other properties remain virtually unchanged. However, the difference in $T_{\rm eff}$ amounts to less than 150 K compared to about 250 K for the $Z = 0.032$ cases discussed so far.

The cooler RGB temperatures imply that the fits to real globular cluster data will have to be reconsidered (they were, in fact, fitting quite well; see Salaris & Weiss 1997, 1998), a deeper look into this is warranted. With the new generation of low-T tables also the opacities for solar mixtures changed slightly (Ferguson et al. 2005), which implies that the solar models need to be recalibrated and the parameter $\alpha_{\rm MLT}$ in the mixing length theory needs some adjustment. Using the Garching stellar evolution code A. Serenelli (private communication, 2006) found that $\alpha_{\rm MLT}$ had to be increased from 1.78 to 1.88. Similarly, for the code used for the models of Fig. 9, a solar calibration (without diffusion) resulted in an increase by 0.12 to the value of $\alpha_{\rm MLT} = 1.95$. Using this value, the dotted track in Fig. 9 results. This would be the completely consistent, correctly calculated track to be used in an update of globular cluster age determinations. Obviously, the new opacity tables along with the consistent $\alpha_{\rm MLT}$ is very close to the AF94-track, and the effect on isochrones is minimal (e.g. effective temperatures differ by 30 K at $\log L/L_sun = 2$), which is a very convenient, but fortunate fact. Thus the globular ages determine in Salaris & Weiss (1998) and Salaris & Weiss (2002) are correct and remain unchanged. We also investigated how a recalibrated $\alpha_{\rm MLT}$ would modify the effect on the more metal-rich effect. This will be reported below and in Fig. 11.

The second aspect to be considered is that of the mixture effect in the high-T opacities (Sect. 3.3), which could affect age determinations of globular clusters by the increased main-sequence lifetimes. The difference in the opacities, going from one α-enhanced mixture to the other, is vanishing with decreasing metallicity (Fig. 10). The difference for the lowest metallicity considered here amounts to less than 3% everywhere. As a consequence, the turn-off ages agree within 200 Myr, or about 2% of the main-sequence lifetime.

The evolution shown in the upper panel of Fig. 9 demonstrates the negligible effect of varying the internal element distribution on the HRD of the $0.8\,M_\odot$ star: at fixed $Z = 0.001$ the three tracks using opacity tables for solar (dash-dotted line), α-v (long-dashed) and α-c (dotted) element ratios are extremely close to each

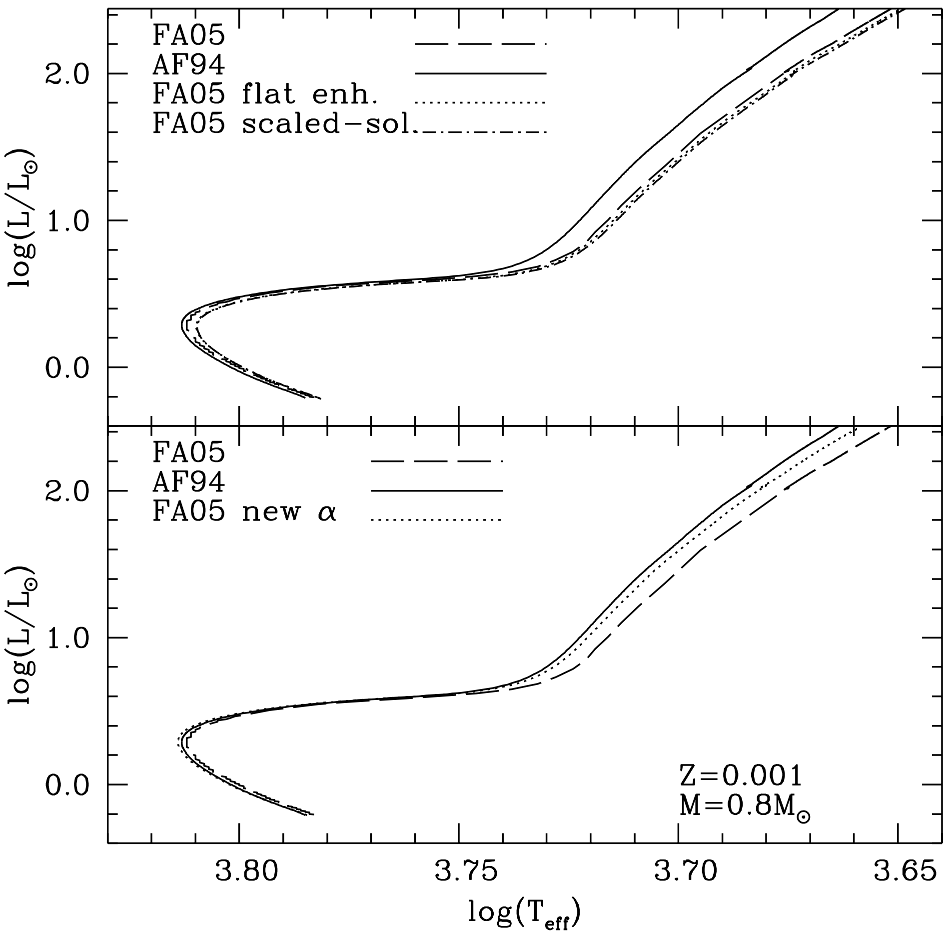

Fig. 9. Lower panel: Evolutionary tracks for an $M = 0.8\,M_{\odot}$ star with $Z = 0.001$ calculated with the original Alexander & Ferguson (1994, AF04) and the new Ferguson et al. (2005, F05) code for the α-v mixture. The dotted line refers to a track with the new opacities, but a recalibrated mixing parameter $\alpha_{\rm MLT}$. Upper panel: Effect of using opacity tables with different internal element distributions but identical Z; see text.

other, the largest – but still very small – effect appearing at the turn-off: The effective temperature agrees for the scaled-solar and α-c mixture within 5 K, while the α-v track is $\approx$ 30K hotter. Luminosities are higher by 0.005 resp. 0.014 dex. This confirms again the results by Salaris et al. (1993). In contrast, the "generation effect" of the AF94 track is much larger. No recalibration of $\alpha_{\rm MLT}$ was done here; this would shift all new tracks in the same way as the dotted one in the lower panel.

Given these results, we return briefly to the super-solar case. In Fig. 11 we compare various cases for two mass values (0.8 and 1.2 $M_{\odot}$). The solid line corresponds again to case B (α-c mixture both in the model and in the opacity tables). The fully equivalent models for the α-v mixture, taken again into account in both model and opacities (Ferguson et al. 2005) is indicated by the dotted line. In both these cases $\alpha_{\rm MLT} = 1.6$. The recalibration of the mixing length parameter yields a value close to 1.7; this case is represented by the dashed line. Finally, case A (model composition α-c, old Alexander & Ferguson 1994 tables, $\alpha_{\rm MLT} = 1.6$) is the most extreme case (dash-dotted line). In contrast to the low-metallicity case, the recalibration of $\alpha_{\rm MLT}$ does not approximate case A. It is also obvious that the change of mixture has its largest effect on the main-sequence due to the increased high-temperature opacities, but less so on along the RGB, where temperatures are much more affected by $\alpha_{\rm MLT}$, which in turn has a smaller effect along the main-sequence, in particular of course for the higher mass with very thin exterior convection zone.

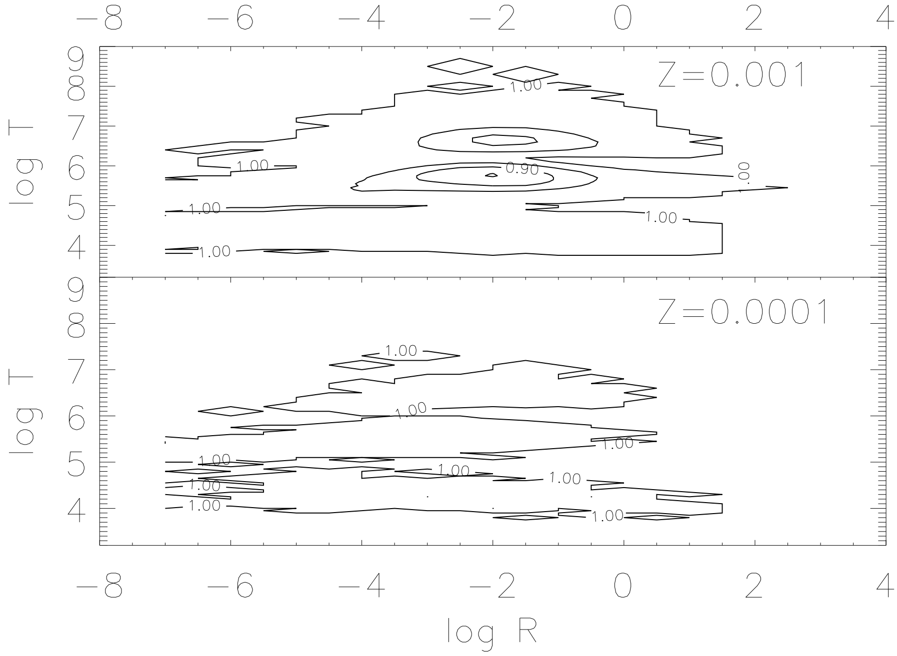

Fig. 10. As Fig. 4, but for Z = 0.001 and 0.0001. X = 0.70 in both panels.

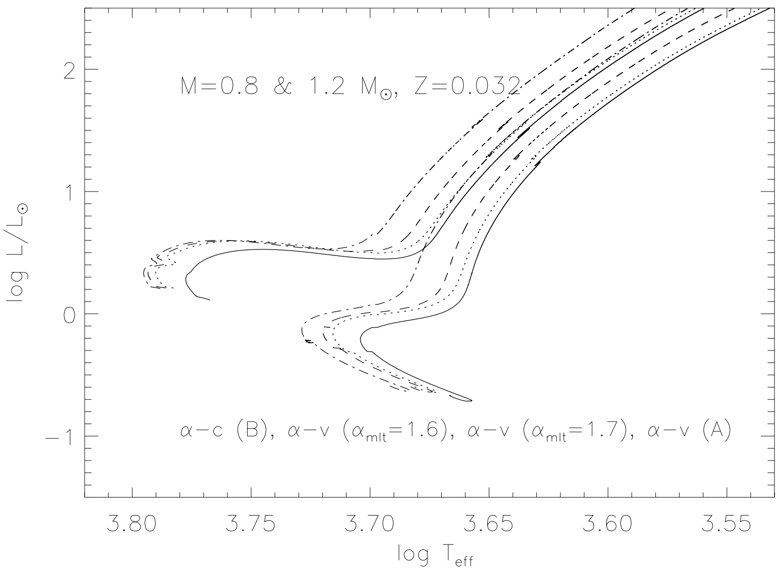

Fig. 11. Overview over various cases for two mass values (0.8 and 1.2 $M_\odot$) for our standard composition of X = 0.679, Z = 0.032. See text for more explanations.

5. Discussion

The diversity of chemical compositions for stellar models will remain to be much larger than that of available opacity tables, which, however are crucial for accurate model calculations. We have therefore investigated how opacities calculated for similar, but not identical α-element enhanced mixtures influence the evolution of stellar models of low mass and super-solar metallicity, where effects are expected to be large. While the models had constant α-enhancement factors (α-c; Table 1) we used tables for the same composition, but also for another one of varying enhancement factors, α-v. The latter opacity tables had been computed about a decade ago with the Alexander & Ferguson (1994) code in response to a specific request.

The initial comparison (Fig. 1) revealed drastic changes in the temperature of red giants and the location and duration of the main sequence. These changes were much larger than what could be expected on the basis of the experience with using solar-scaled mixture opacities instead of α-enhanced ones (Salaris et al. 1993; Salaris & Weiss 1998).

The origin of low- and high-temperature opacities differing, we selectively replaced them to identify the cause for the differences found. The lower stellar temperatures found in case of α-c opacity tables are, in particular along the RGB, almost exclusively due to the low-T molecular opacities (Ferguson et al. 2005), while the main sequence luminosity and thus lifetime varies with the composition of the (OPAL-)high-T tables, the latter by up to 20%! As the code computing the latter tables has not changed since Iglesias & Rogers (1996), this was identified as a pure composition effect: The α-c opacities, for given (X, Z), is consistently higher in a temperature and density range covering the whole energy producing core of low-mass main-sequence stars, which explains the lower luminosity found. We have performed various tests to make sure that we obtained and used the correct tables and have thus verified that the *individual α-element abundances play a significant role for the opacities at stellar core temperatures*. In addition, we created opacity tables for the same mixtures using the latest Opacity Project data (Badnell et al. 2005; Seaton 2005). While in the interesting temperature range the OP Rosseland mean opacities differ from the OPAL ones, the *differential* effect going from α-v to α-c abundance ratios is very similar. If the opacities we have been using are confirmed to be true, the conclusion is far-reaching: at solar- and super-solar metallicities, the lifetime of α-enriched low-mass stars is sensitive to the individual abundance pattern. Accurate age determinations of stars or stellar systems, such as elliptical galaxies or of the galactic bulge, may require very detailed knowledge about the chemical composition.

For the low-T opacities we further had to discriminate between the composition and the generation effect, as the α-c tables had been computed with the recent Ferguson et al. (2005) code. As the result of our tests we discovered that the original α-v tables suffer from an error and are incorrect. Recomputations using both the new and the old Wichita State molecular opacity code resulted in very similar opacities, which, when used (Sects. 3.4 and 3.5), yield much lower RGB temperatures.[4]

The conclusion of our investigation is that at high metallicities both the error in the old low-T tables and the composition details in the high-T opacities significantly influence our models. Previous calculations using the erroneous tables at solar metallicities should be repeated with the new tables for the same α-v composition. For sub-solar metallicities both effects tend to decrease, and in particular for typical Pop. II compositions variations in individual element abundances are no longer significant for lifetimes. Age determinations of globular clusters are thus independent of composition details. We therefore confirm once again the basic results of Salaris et al. (1993). The erroneous low-T tables, in contrast, still render the tracks too hot on the RGB, such that colour-based age determinations would be affected (yielding ages too low). Incidentally, however, a recalibration of the mixing length parameter $\alpha_{\rm MLT}$, which may be considered necessary when using the new low-T tables of Ferguson et al. (2005) almost recovers the old RGB temperatures (Fig. 9, lower panel).

To summarize, we found that metal-rich low-mass stellar models are very sensitive to details of the chemical composition used in opacity tables. It is therefore advisable to employ opacity tables consistent with the assumed stellar chemical composition. The range of massive stars still needs to be investigated. For population synthesis models of metal-rich galaxies knowledge about the mean α-enrichment may not be sufficient for any reasonable statements about the star formation history.

Acknowledgements. JF acknowledges support from NSF grant AST-0239590 with matching support from the State of Kansas and the Wichita State University High Performance Computing Center funded by NSF grants EIA-0216178 EPS-0236913.

[4] The old opacity tables for this mixture have been removed from the web-site `http://webs.wichita.edu/physics/opacity/` and replaced by new calculations.

References

Alexander, D. R. & Ferguson, J. W. 1994, ApJ, 437, 879
Badnell, N. R., Bautista, M. A., Butler, K., et al. 2005, MNRAS, 360, 458
Bencivenni, D., Castellani, V., Tornambé, A., & Weiss, A. 1989, ApJS, 71, 109
Cassisi, S., Salaris, M., & Irwin, A. 2003, ApJ, 588, 862
Ferguson, J. W., Alexander, D. R., Allard, F., et al. 2005, ApJ, 623, 585
Grevesse, N. & Sauval, A. J. 1998, Space Sci. Rev., 85, 161
Huebner, W. F., Merts, L., Magee, N. H., & Argo, M. F. 1977, Astrophysical Opacity Library, Scientifical Report LA-6760-M, Los Alamos Scientific Laboratory
Iglesias, C. A. & Rogers, F. J. 1996, ApJ, 464, 943
Itoh, N., Mitake, S., Iyetomi, H., & Ichimaru, S. 1983, ApJ, 273, 774
Rogers, F. J., Swenson, F. J., & Iglesias, C. A. 1996, ApJ, 456, 902
Salaris, M., Straniero, O., & Chieffi, S. 1993, ApJ, 414, 580
Salaris, M. & Weiss, A. 1997, A&A, 327, 107
Salaris, M. & Weiss, A. 1998, A&A, 335, 943
Salaris, M. & Weiss, A. 2002, A&A, 492
Salasnich, B., Girardi, L., Weiss, A., & Chiosi, C. 2000, A&A, 361, 1023
Seaton, M. J. 2005, MNRAS, 362, L1
Spaeth, H. 1973, Spline-Algorithmen zur Konstruktion glatter Kurven und Flächen (München: Oldenburg-Verlag)
VandenBerg, D. A., Swenson, F. J., Rogers, F. J., Iglesias, C. A., & Alexander, D. R. 2000, ApJ, 532, 430
Weiss, A., Peletier, R. F., & Matteucci, F. 1995, A&A, 296, 73
Weiss, A. & Schlattl, H. 2000, A&A Supplement, 144, 487
Weiss, A., Serenelli, A., Kitsikis, A., Schlattl, H., & Christensen-Dalsgaard, J. 2005, A&A, 441, 1129
Wheeler, J. C., Sneden, C., & Truran, J. W. 1989, Ann. Rev. Astron. Astroph., 27, 279
Yi, S., Kim, Y.-C., & Demarque, P. 2003, ApJ Suppl. Ser., 144, 259